International Journal of System Dynamics Applications
Volume 11 • Issue 6

A 2D Histogram-Based Image Thresholding Using Hybrid Algorithms for Brain Image Fusion

Srikanth M. V., Gudlavalleru Engineering College, Gudlavalleru, India
V. V. K. D. V. Prasad, Jawaharlal Nehru Technological University, Kakinada, India
K. Satya Prasad, Jawaharlal Nehru Technological University, Kakinada, India

ABSTRACT

In this article, an effort is made to identify brain tumor disease such as neoplastic, cerebrovascular, Alzheimer's, lethal, sarcoma diseases by successful fusion of images from magnetic resonance imaging (MRI) and computed tomography (CT). Two images are fused in three steps: the two images are independently segmented by hybrid combination of particle swam optimization (PSO), genetic algorithm, and symbiotic organisms search (SOS) named as hGAPSO-SOS by maximizing 2-dimensional Renyi entropy. Image thresholding with 2-D histogram is stronger in the segmentation than 1-D histogram. The segmented regions with scale invariant feature transform (SIFT) algorithm are removed. Also, after image rotation and scaling, the SIFT algorithm is excellent at removing the features. The fusion laws are eventually rendered on the basis of type-2 blurry interval (IT2FL), where ambiguity effects are reduced unlike type-1. The uniqueness of the proposed study is evaluated on specific data collection of benchmark image fusion and has proven stronger in all criteria of scale.

KEYWORDS

Entropy, Feature Transform, Genetic Algorithm, Image Fusion, Interval Type-2 Fuzzy, Particle Swarm Optimization, Symbiotic Organisms Search

INTRODUCTION

Diagnosing an illness is an essential step toward treating an illness. There are a number of screening methods and medical imaging is one of those. It is a technique for creating a conceptual image of the human body's ideal component including muscles, bones, and brain. To do this several multi-modal medical imaging technologies have been implemented. Image fusion is the principal solution among them. Collecting and fusing necessary information from different images into a composite image, without distortion and detail loss. Image fusion has several benefits, including less confusion, enhanced precision, image sharpening, improvement of characteristics, better recognition, early stage detection of illness, simple to read, low expense, minimized data transfer and color fused image. Image fusion may be used in medical care, space imagery, identification and classification of artifacts, and military.

For image fusion, different techniques and different classifications have been proposed in literature. The important techniques which are depends on image spatial domain (Ghassemian, 2016), techniques using any DWT or DCT transform (Jin et al., 2017), technique with contrast, morphological and ratio pyramids (Petrovic & Xydeas, 2004), technique with Laplacian pyramid

DOI: 10.4018/IJSDA.20221101.oa3

(Yang et al., 2009), techniques depends related to image fusion in pixel level (Naidu & Rao, 2008), techniques based on image feature (Naidu & Rao, 2008), techniques based on decision level (Al-Tayyan et al., 2017). The fusion method for the spatial domain image interacts specifically with the pixels of the reference image. This approach can be evaluated in four ways: principal component analysis (PCA) (Wan et al., 2013), Intensity hue saturation (IHS), clear average, and clear maxima. They may have some drawbacks while they are really useful techniques. An easy maximum creates images that are strongly oriented but it induces blurring (Xu, 2014). Blurring may influence spatial contrast. Simple averaging is not capable of providing direct images of the target but is the easiest tool for image fusion. According to the principal variable research method, spectral loss exists. Saturation of saturation hues is only appropriate for color image fusion, so it is applied for medical imaging applications (Haddadpour et al., 2017).

In case of techniques depends on transform techniques, the image is transformed from spatial to frequency domain and the resultant frequency coefficients are fused to get fused image of two images. To get back spatial fused image apply inverse transform. In these techniques, images are converted to multi-scale or multi-resolution representation before fusion. These techniques covert images by using discrete time wavelet transform (DT-DWT), Complex WT (CWT), Curvelets (Choi et al., 2005), additive wavelets, non-sub sampled Contourlet transform (NSCT) which is used for generates edges, complex contours and textures (Majhi, 2018). Among all, some techniques in transform domain are very better than spatial techniques in few measuring aspects. The very important, discrete wavelet transform can able to handle curved edges which leads fail in fusing brain images in effective way. These techniques have very bad shift sensitivity, directionality, less spatial resolution and destruction of phase information and because of down-sampling effect there may be chance of Pseudo-Gibbs effect. Where as in Curvelet transform, which are good in handling curved edges and capturing curvilinear. So it is best suitable for brain image fusion at the cost of bearing expansive process and consumes more time in execution. In similar, DT-CWT techniques overcome all the drawbacks occurred with spatial and transforms domain with considerable drawbacks. DT-CWT techniques are good in perfect identification of edges, obey property of shift invariance, and take less time in exaction and better directionality properties (El-Hoseny et al., 2018).

The Pyramid techniques are well suitable very specific images for fusion. So, pyramid level image fusion techniques generates only one band-pass image which leads to blocking effects. In addition to this, contrast pyramid techniques lost some important information and Morphological pyramid techniques are bad in edge identification. The pulse coupled neural network (PCNN) technique is good for image enhancement, segmentation and face and pattern recognition. It depends on biological background of human beings. PCNN has a capacity to extract segmentation, enhancement for images at more contrast, clear and huge data. The multi-channel PCNN (M-PCNN) is used for different images fusion at a time and depends on the actual requirement and number of channels can be changed easily. Even though it carries some drawbacks, it is hard and complex to fix the design requirements, and they should adjust manually or they are estimated through huge training. However, here much importance is required in case of parameter selection. So, one should take much importance in selected parameters. The PCCN technique performance depends on these parameters and outcome depends on these. These drawbacks are overcome in image fusion; one can go with optimization techniques. Those include PCNN with cascaded combination of Genetic Algorithms (GA), particle swarm optimization (PSO), extension of PSO (QPSO), FOA and MDE (Lang & Hao, 2014). The pixel level can contain significant quantities of details, and is also extremely accurate. The region could approach by which image fusion can be achieved at pixel level. We are a commonly utilized multi-resolution measurement, color hue saturation, key feature measurement.

We will regard other criteria such as energy, direction, different edges of images, illuminations and many more in order to determine an image fusion technique is right perfect for applications related to image fusion. Since we have determined the strategy we are going towards strategies of global optimisation. Global optimisation is a process for seeking the right selection of qualifying conditions

Figure 1. Block diagram of proposed technique

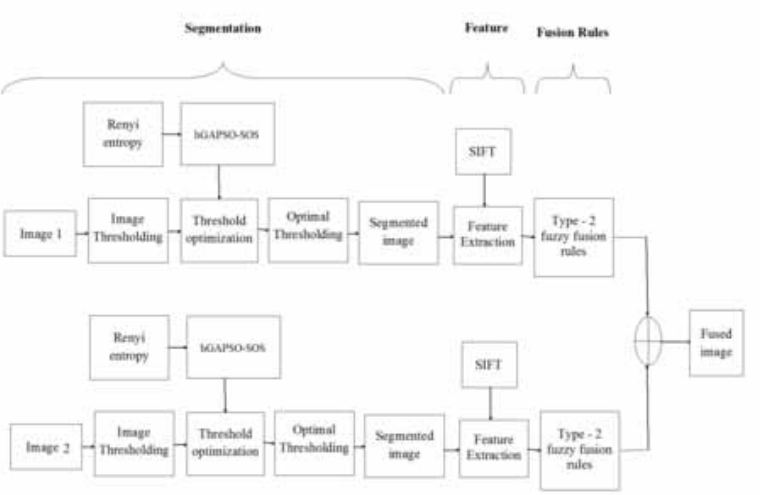

to accomplish our aim. For continuous and discrete functions it is used to locate the maxima and minima. These techniques include (PSO) Chiranjeevi & Jena 2017), gray wolf (GWO) Karri & Jena, 2016), Symbiotic Organisms Search (SOS), firefly algorithm (FA), Honey bee mate (HBMO), Genetic Algorithm (GA) (Chiranjeevi & Jena, 2018; Rokbani et al., 2020). Among these, hybridization of GA, PSO and SOS (hGAPSO-SOS) found more advantageous includes simple implementation, easy mathematics, high computational time and ensuring at high speed of execution. By understanding these image fusion techniques, we consternated on quality of fused image and visually better visualization.

MATERIALS AND METHODS

A region based feature level image fusion is suggested in this article, whereby the regions of two images which are fused and are obtained through suitable or very regional image segmentation. The photos are segmented by optimum criteria for the detection of specific regions or areas in two images. By considering Renyi entropy as a fitness function, the desired values are calculated using appropriate optimisation techniques. Those levels are adjusted depending on the image to be fused in 2-D histogram. The optimisation technique job is to optimize the fitness function which leads to an optimal threshold, henceforward upgraded input image segmentation. The thresholds are modified with the hGAPSO-SOS, and several other state-of-the-art optimisation approaches compared the tests. Upon efficient segmentation of both images, the function of the input images is extracted using the correct extraction techniques for the object. The attributes of an image are in general shape, base, and contour. In this article, image features are retrieved with the Scale Invariant Feature Transform (SIFT) algorithm, it was discovered by David Lowe in 1999 (Lowe, 1999) and the algorithm's working principle begins with the random elimination of artifacts from the reference image and the identification of new objects from other images on the basis of the minimum Euclidean distance between the reference and the item to be identified. Detailed algorithm summary can be contained in reference number (He et al, 2018). The separated features of both images are fused according to the principles of type-2 Fuzzy Fusion. Zadeh (1965) developed Fuzzy set theory in 1965. This is observed, however, that type-1 fuzzy set is not versatile and scalable, thus, a type -2 fuzzy set is likewise introduced, and in which membership function is unclear due to ambiguity in membership

relationship. And it can be tailored to both definite and unknown issues. The block diagram of the suggested algorithm is seen in Figure 1.

Image thresholding: One image clustering strategy is pixel thresholding. Because of its easy and modular design it is used in many applications such as machine vision, data gathering, data segmentation etc. Image thresholding can be either bi-level or multi-level, while in the first example two thresholds are used to divide the image into three regions. Whereas in the second case, the user determines the number of thresholds according to his requirement. If 'c' is the number of threhsholds then 'c+1' is the number of clusters or fragments. The segmented result depends on perfect threshold positioning that segment the input image. Placing those thresholds for different images is a difficult task. Those thresholds are then optimized with hGAPSO-SOS by treating Renyi entropy as an objective function in this paper. A quick overview of hGAPSO-SOS, Renyi entropy, Type-2 Fuzzy, Scale-Invariant Feature Transform, and Fusion Rules will be addressed in the following sub part.

Overview of Renyi Entropy

Let's assume an 'n' array finite discrete probability distributions (pdf) such as (F_1, F_2, F_3, …… F_n) ε Δ_n where Δ_n = {(F_1, F_2, F_3, …… F_n), F_i ³ 0, i = 1, 2, 3…..n, n ³ 2, } with random variables (X_1, X_2, X_3, …… X_n) then Renyi entropy for independent and additive random events is given as (Galli, 2018).

$$H_\alpha = \frac{1}{1-\alpha}\log_2\left(\sum_i^n F_i^\alpha\right) \tag{1}$$

Where 'α' entropy order which is greater than zero. When 'α' is almost equal to one, then Renyi becomes Shannon entropy. In general images are clustered in to two, one always carries object information (cluster C_1) and second carries background (cluster C_2), and then Renyi entropy is given as

$$H_\alpha\left[C_1\right] = \frac{1}{1-\alpha}\left[\log_2\left(\sum_{i=0}^{t}\left(\frac{F\left(i\right)}{F\left(C_1\right)}\right)^\alpha\right)\right] \tag{2}$$

$$H_\alpha\left[C_2\right] = \frac{1}{1-\alpha}\left[\log_2\left(\sum_{i=t}^{L-1}\left(\frac{F\left(i\right)}{F\left(C_2\right)}\right)^\alpha\right)\right] \tag{3}$$

Where $F\left(C_1\right) = \sum_{i=0}^{t} F\left(i\right)$, $F\left(C_2\right) = \sum_{i=t+1}^{L-1} F\left(i\right)$, Here 'L' is highest intensity level of gray scale image and F_i is the one dimensional normalized histogram of the image. The overall Renyi entropy with one threshold 't' of given image is

$$\varphi_\alpha\left(t\right) = argmax\left(\left[H_\alpha\left[C_1\right] + H_\alpha\left[C_2\right]\right]\right) \tag{4}$$

Multi-Level Thresholding: Let image is divided into 'N' number of clusters $C = (C_1, C_2, C_3, \ldots\ldots C_N)$ with N number of threshold values $t = (t_1, t_2, t_3, \ldots\ldots t_N)$ then Renyi entropy for each individual cluster is defined as [21]

$$H_{\pm}\left[C_1\right] = \frac{1}{1-\pm}\left[\log_2\left(\sum_{i=0}^{t_1}\left(\frac{F\left(i\right)}{F\left(C_1\right)}\right)^{\pm}\right)\right] \tag{5}$$

$$H_{\pm}\left[C_2\right] = \frac{1}{1-\pm}\left[\log_2\left(\sum_{i=t_1+1}^{t_2}\left(\frac{F\left(i\right)}{F\left(C_2\right)}\right)^{\pm}\right)\right] \tag{6}$$

$$H_{\pm}\left[C_N\right] = \frac{1}{1-\pm}\left[\log_2\left(\sum_{i=t_N-1}^{L-1}\left(\frac{F\left(i\right)}{F\left(C_N\right)}\right)^{\pm}\right)\right] \tag{7}$$

Where $F\left(C_1\right) = \sum_{i=0}^{t_1} F\left(i\right)$, $F\left(C_2\right) = \sum_{i=t_1+1}^{t_2} F\left(i\right)$, $F\left(C_N\right) = \sum_{i=t_N-1}^{L-1} F\left(i\right)$, the overall Renyi entropy or objection function for a given image for N thresholds is given as

$$\varphi_{\alpha}\left(t\right) = argmax\left(\left[H_{\alpha}\left[C_1\right] + H_{\alpha}\left[C_2\right] + \ldots\ldots\ldots H_{\alpha}\left[C_N\right]\right]\right) \tag{8}$$

For simplifying the calculations, two dummy thresholds are introduced t_0 and t_N = L-1 which satisfy the condition $t_0 < t_{1\ldots\ldots\ldots} < t_{N-1} < t_N$. The optimal thresholds are obtained by maximizing the above equation with optimization technique.

Two-Dimensional Renyi Entropy: Let I(*m,n*) is an intensity of an image at location (*m,n*). Digital image [*I*(m,n)| *m* ε {1, 2, 3,……., *M*}, n ε {1, 2, 3,……., *N*}, where '*M*' and '*N*' are dimensions of the image and 1D-histogram h(x) for *x* ε {1, 2, 3,……., *L-1*}, where '*L*' maximum intensity is equal to 256 for gray scale image. Let denote elements in histogram {1, 2, 3… 255} as G. As per literature, optimal thresholds are selected based on 1D-histogram and are optimized by objective function/entropy.

The 2-D histogram of an image is obtained by defining a local average of pixel, *I*(*x,y*), as the average intensity of its nine neighbors denoted as *g*(*x,y*) (Sarkar & Das, 2013)

$$g\left(x,y\right) = \frac{1}{9}\sum_{i=-1}^{1}\sum_{j=-1}^{1} f\left(x+i, y+j\right) \tag{9}$$

Figure 2. Example for 2-D histogram calculation

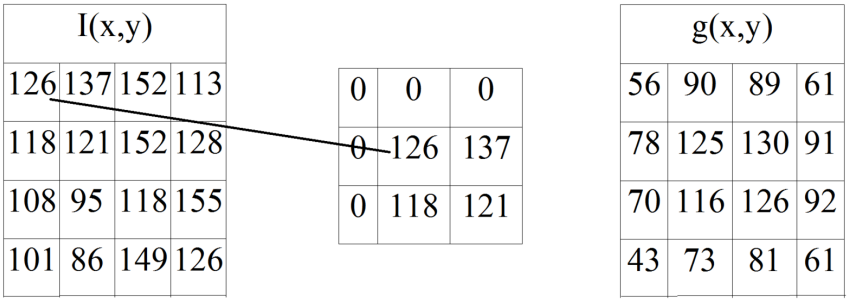

For eg, let's take an image of size 4 * 4 as shown in figure 2(a) and measure its average intensity g(x, y) by padding the necessary number of edge zeros as shown in figure 2(b). First table in figure is image and first dimension i.e. 126, g(x, y) is determined by padding zero's at edges as seen in figure and last tables g(x, y) for entire I(x, y). The 2-D Lena image histogram at defined region as seen in Figure 3, where diagonal quadrants provide a lot of details.

Figure 3 shows the 2-D histogram of the tested images and is divided by a single threshold (t, s) into four clusters. Where t is I(x, y) threshold for initial image intensity and s is g(x, y) threshold for average image intensity. The divided area of the cluster is not identical. The diagonal quadrant 1st represents the target and the 3rd represents the backdrop and the 2nd and 4th quadrants are ignored as it does not provide any details as seen in the diagram. For object and context, the Renyi entropy is given as

Figure 3. Lena image and 2-D histogram

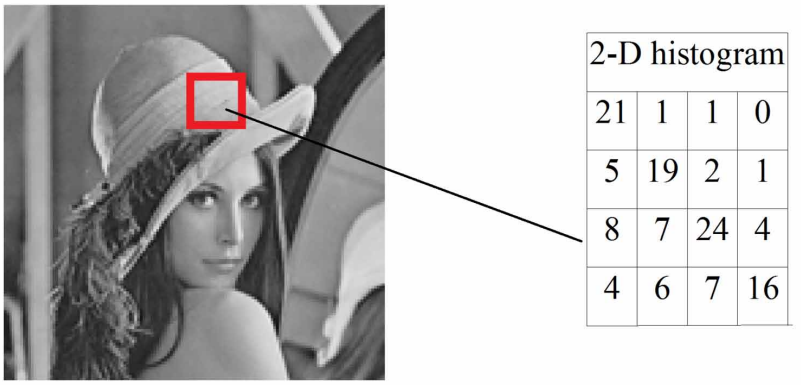

$$H_{object}^{\alpha}[t,s]=\frac{1}{1-\alpha}\left[\log_2\sum_{i=0}^{t}\left(\sum_{j=0}^{s}\left(\frac{F(i,j)}{F_{D1}(t,s)}\right)^{\alpha}\right)\right] \tag{10}$$

$$H^{\alpha}_{background}\left[t,s\right]=\frac{1}{1-\alpha}\left[\log_2\sum_{i=t+1}^{L-1}\left(\sum_{j=s+1}^{L-1}\left(\frac{F\left(i,j\right)}{F_{D2}\left(t,s\right)}\right)^{\alpha}\right)\right] \tag{11}$$

Where $F_{D1}\left(t,s\right)=1-\sum_{i=0}^{t}\sum_{j=0}^{s}F\left(i,j\right)$ and $F_{D2}\left(t,s\right)=1-\sum_{i=t+1}^{L-1}\sum_{j=s+1}^{L-1}F\left(i,j\right)$

The final objective function which is to maximized for better threshold (*t*,*s*) selection is

$$\varphi_{\alpha}\left(t\right)=argmax\left(\left[H^{\alpha}_{object}\left[t,s\right]+H^{\alpha}_{background}\left[t,s\right]\right]\right) \tag{12}$$

Proposed Renyi 2d-Hisotgram Based Multi-Level Thresholding

The major problem with 1-D histogram based thresholding is that distribution of information is all over the range (0 to 255). Our study confirmed that, two dimensional thresholding of input images gives more information about them and especially much information is occupied in particular region. So it's very easy to place threshold depends on information concentration regions and non-concentrated regions. In this paper we suggested a multilevel entropy dependent 2-D Renyi threshold for image segmentation by integrating the 2-D histogram benefit. If the image's 2-D histogram is clustered into 9 clusters with two thresholds (t_1, t_2) and (s_1, s_2) as seen in the figure 4 (a). The quadrants of figures 4, first, fifth and ninth reflect artifacts, transitional regions and context regions respectively. The Renyi's entropy of diagonal is calculated with following equations.

$$H^{\alpha}_{object}\left[t,s\right]=\frac{1}{1-\alpha}\left[\log_2\sum_{i=0}^{t_1}\left(\sum_{j=0}^{s_1}\left(\frac{F\left(i,j\right)}{F_{D1}\left(t,s\right)}\right)^{\alpha}\right)\right] \tag{13}$$

$$H^{\alpha}_{intermediate}\left[t,s\right]=\frac{1}{1-\alpha}\left[\log_2\sum_{t_1+1}^{t_2}\left(\sum_{s_1+1}^{s_2}\left(\frac{F\left(i,j\right)}{F_{D2}\left(t,s\right)}\right)^{\alpha}\right)\right] \tag{14}$$

$$H^{\alpha}_{backgroud}\left[t,s\right]=\frac{1}{1-\alpha}\left[\log_2\sum_{t_2+1}^{L-1}\left(\sum_{s_2+1}^{L-1}\left(\frac{F\left(i,j\right)}{F_{D3}\left(t,s\right)}\right)^{\alpha}\right)\right] \tag{15}$$

Where $F_{D1}\left(t,s\right)=1-\sum_{i=0}^{t_1}\sum_{j=0}^{s_1}F\left(i,j\right)$, $F_{D2}\left(t,s\right)=1-\sum_{i=t_{1+1}}^{t_2}\sum_{j=s_1+1}^{s_2}F\left(i,j\right)$ and

$F_{D2}\left(t,s\right)=1-\sum_{i=t_{2+1}}^{L-1}\sum_{j=s_2+1}^{L-1}F\left(i,j\right)$

Finally, fitness function that is to be maximized for selection of better threshold vales (*t*,*s*) is

$$\varphi_{\alpha}\left(t\right) = argmax\left(\left[H^{\alpha}_{object}\left[t,s\right] + H^{\alpha}_{intermediate}\left[t,s\right] + H^{\alpha}_{background}\left[t,s\right]\right]\right) \tag{16}$$

Now extend equation 16 for user defined number of threshold 'N'

$$\varphi_{\alpha}\left(t\right) = argmax\left(\left[H^{\alpha}_{1}\left[t,s\right] + H^{\alpha}_{2}\left[t,s\right] + H^{\alpha}_{3}\left[t,s\right]\ldots\ldots\ldots\ldots H^{\alpha}_{N+1}\left[t,s\right]\right)\right) \tag{17}$$

$$\text{Where } H^{\alpha}_{k}\left[t,s\right] = \frac{1}{1-\alpha}\left[\log_{2}\sum_{i=t_{k-1}+1}^{t_{k}}\left(\sum_{j=s_{k-1}+1}^{s_{k}}\left(\frac{F\left(i,j\right)}{F_{Dk}\left(t,s\right)}\right)^{\alpha}\right)\right] \tag{18}$$

Let's take two user defined temporary threshold t_0 and t_N+1= L-1 with the condition that $t_0 < t_{1.....} < t_{N-1} < t_N+1$ and another two user defined temporary constant variables s_0 and s_N+1 = L-1 1 with the condition that $s_0 < s_{1.....} < s_{N-1} < s_N+1$ for calculating the entropy to a particular given input image. Figure 5 display the two dimensional histogram of given four input images from various database. From the figure, maximum peaks and minimum peaks are occurred along with quadrants diagonal and vertical respectively. From the fact that, time of convergence or execution time in producing the optimal thresholds depends on user defined number of thresholds 'N'. One solution to this is, utilization of optimization algorithms which reduce convergence time and improve fusion results.

OVERVIEW OF HYBRID GA-PSO-SOS (HGAPSO-SOS):

Genetic Algorithms (GA): It was initiated and developed between the years 1960s to 1970s by team called Holland team and had been using for many constrained and unconstrained optimization problems. It is inspired and developed by in depth study of natural selection of Charles Darwin's theory (Saafan et al., 2017). It is a non-swarm based optimization technique for optimization of any problem and was developed by observing the human intelligence and cause for the difference in intelligence. It is proved that GA can solve any problem which may be any four combinations between continuous, linear, discrete and non-linear. GA being a non-swarm based technique consists of chromosome for each and every population or solution of the problem. These chromosome may be represented in two ways. First one binary representation where all the solutions and operations are in the form of binary digits and second one floating point where all functions are in floating point numbers. Floating points includes real numbers where all the real numbers and dimensions of the problem is equal to the number of variables which are to be optimized. Initial population are generated by a random numbers with in the range of search space and are depends on the maximum and minimum value of parameters to be optimized. Now select a best solution based on the fitness function and generate a new population with any four selection methods those are Fitness proportional, Ranked based, Tournament and Roulette wheel selection. The ordinary GA uses two steps for selection and creation of new population i.e mutation operation and crossover operation. The newly generated population or chromosomes are named as offspring (Grosan & Abraham, 2011). The crossover operation is performed between two parents for generation of new healthy child. The crossover operation is performed based on two assumptions:

Figure 4. 2-D histogram for a) 3- level b) 4- level.

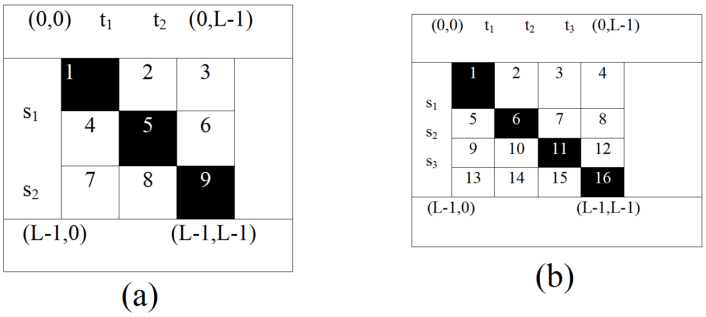

Figure 5. Input images and corresponding 2-D histogram

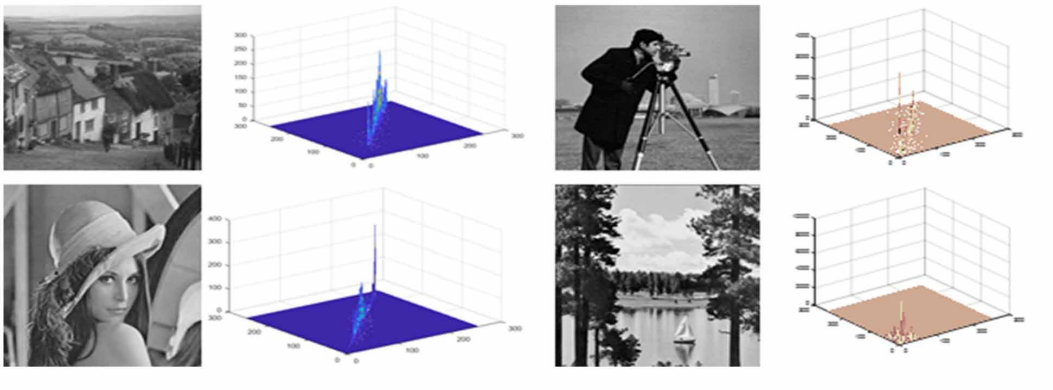

- All the operations are in discrete form and all obey the binary operation rules.
- Assigning new real values using operators for offspring position that goes in-between parent values. These calculations are given as intermediate or arithmetic recombination. Let A and B are the parents then offspring C is computed with the following equation

$$C_i = \alpha \cdot A_i + (1 - \alpha). B_i \; \alpha \hat{I} [0, 1] \tag{19}$$

In all iterations chromosomes changes its values by mutation operation. This operation is applied on chromosome parent for generation of new offspring. Like crossover, mutations also have some variants based on chromosome. Mutation in real number is obtained by addition of chromosome with randomly created real number or randomly generated number from Gaussian (normal) distribution. Let A is chromosome and its i^{th} variable is A_i then new offspring A^l is obtained by mutating i^{th} gene Ai^l and is calculated with the following equation:

$$Ai^l = A_i + N, N = \text{rand } (0, 1). [UB - LB / M], LB < A_i \text{ and } Ai^l < UB \tag{20}$$

Where 'N' is random number or value taken form Gaussian distribution and 'M' is random real number (range between 1 and 1000 (mostly authors prefer M value 10). rand (0,1) is a random number lies between 0 to 1. LB and UB are upper limit and lower limit of A_i and A_i^1. The GA algorithm is represented in algorithm 1.

Algorithm 1: Genetic algorithm

Step 1: Initialize number of chromosome as N.
Step 2: Calculate the objective function/fitness function for all N chromosome.
Step 3: N chromosome are updated by four repeated steps i.e best chromosome selection – Crossover operation and Mutation operation and finally Replacement
Step 4: The generated chromosome are forwarded for next iterations
Step 5: Repeat step 2 - 4 till stopping criteria or maximum iteration

Particle swarm optimization: It is inspired by the searching behavior of particles; some examples are swarm of fish or birds and were developed in the year 1995 by Eberhart and Kennedy (Mousa et al., 2015). Unlike GA, the PSO does not go throw crossover and mutation instead it follows randomness and some intelligence in updating of the both particle positions and velocity. The PSO being a swarm based optimization and is simple and easily adopted for any particle and mathematical problems. While searching for answer to any problem it follows a specific strategy. Each particle in PSO may be assumed as one bird or one fish and are indicated with O_i . All particles always try becoming a best among and changing their positions with a specific strategy. In beginning, some number of populations are initialized which search entire search space. Each particle gain some initial velocity V_i and position Q_i of dimensions equal to dimensions of the problem. In all iterations each particle hold some position called personal best (O_p) and highest fitness particle holds global best (O_{best}) position and these positions are updated in upcoming iterations.

Let 't' is current iteration, then PSO velocity and position update follows Eq 21 and Eq. 22

$$V_{i,d}(t+1) = V_{i,d}(t) + c_{1*}r_1(O_{p(i,d)}(t) - O_{i,d}(t)) + c_{2*}r_2(O_{best(d)}(t) - O_{i,d}(t)) \quad (21)$$

$$O_{i,d}(t+1) = O_{i,d}(t) + V_{i,d}(t+1) \quad (22)$$

Eq. (21) is for velocity updation and Eq. (22) is for updation of particle position with the help of updated velocities. $O_{p(i,d)}$ is a personal best for the d^{th} dimension of particle I and O_{best} is the best particle among all particle in current iteration 't', c_1 and c_2 are user defined control tuning parameters, r_1 and r_2 are random numbers lies between 0 to 1. The PSO algorithm is represented in algorithm 2.

Symbiotic Organisms Search (SOS): SOS is soft computing techniques developed based on organisms and was proposed in the year 2014 by Prayogo and Cheng, it is inspired from symbiotic organisms which are used to survive in nature (Cheng & Prayogo, 2014). SOS is developed for continuous search space. The projected SOS algorithm tries to pursue the fitness organism and simulates symbiotic behavior interactive amongst the paired organism relationship in the ecosystem. The individuals in the population are known as organism and every organism signifies a point in the search space, hence obtaining the possible optimal global solution is achieved to the problem. The fitness for every organism shows the degree of adaption to the treated goal. This algorithm has various advantages over the other algorithms such as: The major advantage of SOS is, it does not

Algorithm 2: PSO algorithm

1: Initialize positions of all particles O_i and corresponding velocities V_i.
2: Assign highest fitness particle as O_{best}
3: While (termination criterion)
4: for i=1, 2,...,n do
5: Update velocities of all particles by using Eq. (21)
6: Update positions of all particles by using Eq. (22)
7: Find new objective function of updated particle $O_i(t + 1)$
8: If new objective function value $O_i(t + 1)$ is higher than old $O_{p,i}(t)$ then
9: Replace $O_{p,i}(t)$ with $O_i(t + 1)$
10: end if
11: end for
12: Now find $O_{best}(t)$ in all updated particles $O_p(t)$
13: itr = itr + 1 (iteration increment)
14: end while
15: Finally outcome O_{best} is generated.

require prior tuning of tuning parameters. As like other algorithms, SOS update the all organism position in each iteration. Position update is done in three successive operations, those are Mutualism/ Commensalism/Parasitism. The organism positions changed based on best possible relation among all. The first step mutualism gives a benefit to both organism as in bees and flowers. The second commensalism gives some value to organism by making a relation between fish and shark. Third one remora gives benefit to shark without the effect the relation with fish. In all phases, the positions are updated if and if relation leads to best objective value for i or j organisms. The above discussion is summarized in algorithm 3.

Algorithm 3: SOS algorithm

1. Initialize the required parameters
2. While (until stopping criterion) do
Three phases 1. Mutualism 2. Commensalism 3. Parasitism
3. End while
4. Each iteration, update the all phases with the corresponding equations Eq. (23) to Eq. (25).

Mutualism phase: in which both the organism are benefited related to the relationship between flowers and bees. In this stage, organism O_j randomly selected and is interact with the other organism O_i. They maintain a good relationship between them so that both organism got benefited. The updated position of both the organism is btained with the following equations.

$$O_{inew} = O_i + \text{rand}\ (0, 1).\ (O_{best} - \text{Mutual\_vector}.\ BF_1) \tag{23}$$

$$O_{jnew} = O_j + \text{rand}\ (0, 1).\ (O_{best} - \text{Mutual\ \_vector.}\ BF_2) \tag{24}$$

$$\text{Mutual\_vector} = O_i + O_j / 2 \tag{25}$$

Where mutal_vector gives relationship between the organisms O_i and O_j and above equation explains the efforts of mutualistic in gaining the their goals and enhance their living survival. The benefit factors BF_1 and BF_2 shows how much of benefit organism acquired while interacting with other organism. These two are randomly selected must be either 1 or 2. O_{best} is the best degree of adaption that has founded until now.

Commensalism phase: This phase is developed on the basis of relation between the Remora fish and sharks. The remora always receives benefits whereas shark may or may not receive benefits from relationship. As disused in mutualism phase, in this randomly selected O_j organism gets benefit by maintaining a relationship with other organism O_i. Then updated equation is (26)

$$O_{inew} = O_i + \text{rand}\ (-1, 1).\ (O_{best} - O_j) \tag{26}$$

Parasitism phase: This phase exit between the human being and malaria mosquito, in which human being got effected and some time may die and mosquito benefited with the relationship. As one of the organisms got effected so need to replace with newly generated organism. As like other phases, one organism is selected randomly O_j and it acts a victim for parasite vector. In problem search space this vector is obtained by replacing O_j with newly generated and then modify the randomly chosen organism. If at all this vector is better as compared to O_j then this phase kill O_j and replace or else O_j gains some energy from parasite and live for some other days.

Hybrid algorithm based on GA, PSO and SOS

Developed by Charles Darwin for the first time by merging of three of the evolutionary algorithms GA, PSO and SOS represented as hGAPSO-SOS, has been taken from natural selection (Chiranjeevi et al., 2017). As per authors view, organisms always try to become strong in life by competent with other organism so all organisms has better probability to propagate and leads to a better offspring. These offspring will receive the features which finished the parents ending well. These features of organisms will spread to all population in search space and this process is called evolution (Naugle et al., 2019). Here is fact that if any organism has good genetic structure leads a better feature, henceforth better and has long life in ecosystem. This kind of behavior leads to better relation with others organism and each organism increase life span and their experiences will be shared to children's for better life. In the proposed algorithm we took the advantage of incorporating the SOS with GA. The GA creates a better offspring with good genetic structure from parents. The PSO algorithm gives some important experiences to all organism which leads better survival of each organism. In the proposed algorithm GA follows PSO and combination follows SOS.

In all iterations, the hGAPSO-SOS starts with GA with required population, dimension of problem and required initialization of parameters. The selection operation of GA is useful for selection of best population which is obtained after doing some required or mandate operations mutation followed by crossover operation. The global best solution Obest is also selected among all populations. The outcome of GA populations is obtained by incorporating parent's experiences and corresponding offspring. There are five parameters in each offspring those are position, velocity, best experience (which itself consists of two fields position and cost) and cost. In next step all organisms get some best experience with PSO. If any organism position is better as compared to past position then it

will move to better level or else it will remain in same position. If best experience is better than the global best Obest then replace it with new position. So PSO always try to check for better position by updating the velocity and keep best for the next iterations and parallelly it update the Obest. As all the organisms got some experience with the PSO, now they try to establish a better relation with other organism which leads to better offspring and healthy population. In third phase, if any organism got improved fitness value then that organism position is updated with SOS interaction if not nothing do. From whole observation the GA and SOS are useful for position update and PSO update the Obest and personal best of organism. If Obest value in current iteration is equal to stopping condition then algorithm stop or else same process is repeated.

SCALE-INVARIANT FEATURE TRANSFORM

Harris feature detectors are invariant to rotation, i.e. the same corners in images are observed both after rotation of the image as before rotation, but when image is scaled it does not detect angles. Corners in an image might or may not be angles after the image has been sized. So this detector function is a version of the scale (Naugle et al., 2019). In the year 2004, the SIFT is implemented to statement this downside. The algorithm goes through four steps:

A. **Scale space peak selection:** Multiple window sizes are used to identify key points in various sized pictures, and this process, called the scale space filtering, generates specific sizes of windows from Laplacian of Gaussian (DoG). Gaussian meaning distinction is determined using two Gaussian images discrepancy.
B. **Key point localization**: After the main points have been successfully defined in the first step, these points are further optimized for accuracy by producing various sizes of windows according to the Taylor series and then find it or fail to take into consideration if the serious strength of the position obtained goes beyond the user-defined threshold. Unlike all other unwanted corners, these positions should be eliminated in the 2x2 hessian matrix as in the Harris corner detector after Gussian feature discrepancy. Only the extreme edges and main points are received after setting step A.
C. **Orientation assignment**: At this point the orientation of the key points is traced based on their gradient height, magnitude and position. This paper includes some 36 bins spanning 360 degrees. The maximal 'H' value is defined by the histogram of an image and is seen in the plotting when the main point intensity exceeds 80% H.
D. **Key point descriptor** (describing the key point as a high dimensional vector): In the three measures above, the principal point descriptor is obtained by means of a local gradient. Gaussian rotates the gradient information obtained to follow the key point path and then tests it with a variance of 1.5 main points. This data is used to construct a series of histograms at the middle of the main level. There are a total of 16 histograms arranged in 4x4 grid shape and 8 instruction bins in each column. This corresponds to a vector of 128. These vectors are referred to as SIFT keys that label picture with the closest line. When, more than three keys qualify for a particular role to be identified for further processing.

TYPE-2 FUZZY SET

The idea named Zadeh's generated as a fuzzy set. Fuzzy set theory primarily addresses the uncertainty-related questions. However, since traditional fuzzy set membership functions of type-1 are defined, the minimization of ambiguity effects is difficult when utilizing any algorithm and membership feature. For functional implementations the membership function is typically empirically founded on experience with a large degree of subjectivity. A generic Fuzzy set suggested by Zadeh to resolve

the above-mentioned issues, i.e. category 2 Fuzzy set. The relationship between membership feature and entity is fuzzy and uncertain in a second form Fuzzy set. Hence, a type-2 fuzzy collection will define the fuzzy uncertainty membership function, and the uncertainty components.

$$B= \{((y, u), \mu_B(y, u))|\forall y \hat{I} Y, \forall u \hat{I}Ky\acute{I} [0, 1]\} \quad (27)$$

Where B corresponds to a type-2, $\mu_B(y, u)$ is referred to as the 0-alternative $\mu_B(y, u)$-allocating feature of the type-2. Ky denotes the $\mu_B(y',u)$ main membership feature while the Y=y' secondary membership feature. Thus the difficulty of type 2 fuzzy set, in which more calculations are needed, is higher than that of type 1. The question comes where secondary engagement functions are regarded. A generalized flushing type-2 collection sometimes used for functional implementations, such as the flushing type-2 interval range (Harris & Stephens, 1988). In Fuzzy set type-2, the membership of the organization is specified as

$$B= \{((y, u), 1)|\forall y \hat{I} Y, \forall u \hat{I}Ky\acute{I} [0, 1]\} \quad (28)$$

An alternative type-2 fuzzy set is defined as (with the help of membership functions of type-1)

$$B = (y, \mu_M(y), \mu_V(y))|\forall y \hat{I} Y\ \mu_M(y) £ \mu(y) £ \mu_V(y)|u \hat{I} [0, 1] \quad (29)$$

Where $\mu(y)$ denotes an initial membership function of thype-1, B is the interval type-2 fuzzy set, and μM (y) and μV (y) is the upper and lower membership functions with respect to upper and lower envelopes of the interval membership function (type-2) and fuzzy set type-1 membership function can be obtained. Practically a pair to characterize reciprocal parameters i.e.,

$$\mu_M(y) = [\mu(y)]\alpha, \mu_U(y) = [\mu(y)](1/\alpha) \quad (30)$$

Where α is a textual shield that is naive (α ³ 1). With α Î [1, 2], strong performance can be achieved. Footprint of ambiguity (FOU) can be expressed by comparing both the fuzzy set type-1 and the fuzzy set type-2 (Dutta, 2017). The form of type-2 fuzzy set used in literature is defined by term FOU, thus FOU gives the distribution at the top of the shaded field.

Fusion Rule

Let's say two images M and R to combine. After efficient segmentation of both images their respective segmented regions are represented as $M : \{ S_{p,q}^{M} \}$ and $R : \{ S_{p,q}^{R} \}$. where p and q represent the segmented regions and their respective pixel locations. The fusion rules play an important part in the success of the proposed method of segmentation. The previously suggested rules for image fusion are sensitive to high frequency noise, i.e. borders, area boundaries and textures (Mendel & John, 2002), but this paper suggests a type 2 fuzzy set that takes local and global image knowledge. *μ()* membership function form is offered as

$$\mu_{p,q}^{I}\left(i,j\right) = \frac{1}{1+\left|\frac{s_{p,q}^{I}\left(i,j\right)-c}{a}\right|^{2}} \quad (31)$$

Where $I = (M, R)$ and (i, j) shows the location of segmented images. Here, c is average of ($s_{p,q}^{I}$) and 'a' is minimum of ($s_{p,q}^{I}$) . Next, at each position of the membership function, lower and upper membership functions $\mu_L(x)$ and $\mu_U(x)$ are calculated as follows:

$$\begin{cases} \mu_L^{I,p,q}\left(x,y\right) = [\mu_{p,q}^{I}\left(i,j\right)]^{\alpha} \\ \mu_U^{I,p,q}\left(x,y\right) = [\mu_{p,q}^{I}\left(i,j\right)]^{1/\alpha} \end{cases} \tag{32}$$

Fuzzy set output is calculated on the basis of Fuzzy entropy, a strong Fuzzy entropy value indicates the strongest Fuzzy set and weak Fuzzy entropy value means Wicked Fuzzy set (Yang et al., 2016). Hence a higher Fuzzy entropy value contributes to stronger laws for image fusion.

RESULTS

The efficiency of the proposed procedure is tested by conducting experiments on five pairs of images related to different brain disorders. In Set-A, CT, and T2- Weighted MR photos of neoplastic disorder associated brain tumor. T2-Weighted MR photos of brain injury in Set-B, CT, attributable to cerebrovascular disorder. In Set-C, the T1-Weighted MR and T2-Weighted brain representations contributing to Alzheimer's disease are portrayed. The T1-Weighted MR and T2-Weighted MR images of the brain linked to fatal disease are illustrated in Set-D, whereas the CT, T1-Weighted MR images of the brain attributable to sarcoma disease are portrayed in Set-E. The medical images used in article are obtained from https://www.imagefusion.org/ and http://www.med.harvard.edu/aanlib/home.html. All simulations are performed on HP Compaq probook 4430s laptop with Matlab version 2016a.

Measuring parameters:

Standard deviation (STD): The gray contrast value in the composite image is the standard deviation. The fused image should be sharply contrasting at the stage where the approximate S is small. When p(k) is a gray level k likelihood, and km is the mean of k (Li & Li, 2008).

$$\text{STD}=\sqrt{\sum_{K=0}^{J-1}\left(k-k_m\right)^2 p\left(k\right)} \tag{33}$$

Structural similarity index (SSIM): The index of structural similarity is used to measure the resemblance or closeness between two images (Li & Li, 2008). Comparing one image given with the other one, it is used to compare accuracy. This is regarded as being of outstanding consistency. It is the updated edition of the standardized index of image efficiency. Find $D1=(m_1N)^2$ and $D2=(m_2N)^2$ as the two variables that will balance the division by having the denominator low. N stands for vector dynamic range prices. The standard m1 and m2 values are 0.01 and 0.03, respectively. If the fused image is 'f' and the reference image is r.

$$SSIM = \frac{\left(2r2f + D1\right)\left(2r2f + D2\right)}{\left(2r2f + D1\right)\left(2r + 2f + D2\right)} \tag{34}$$

Table 1: Set –A: Neoplastic disease

Method	FSIM	ENTROPY	PSNR	SSIM	STD	$Q^{AB/F}$	MI	CC
PSO	0.893427	21.064733	34.32786	0.91319	0.189056	0.620952	3.23917	0.62095
QPSO	0.956501	21.109136	34.36472	0.914872	0.206056	0.663134	3.28259	0.66313
HBMO	0.958995	21.134748	34.38426	0.934355	0.234453	0.683590	3.28660	0.68359
Proposed	0.989454	21.423541	34.39587	0.958789	0.240123	0.654544	3.30002	0.69541

Mutual information (MI): Mutual information is used as a metric for recognizing success in multimodal fusion (Bhateja et al., 2015). When the MI meaning is strong than it means that parental image detail is limited by the merged frame. P(m), p(n) is the median probability distribution function of both images; p(m, n) is the sum of the combined probability distribution.

$$MI\left(m,n\right)=\sum_{m\in M}\sum_{n\in N}p\left(m,n\right)log\left(\frac{p\left(m,n\right)}{p\left(m\right)p\left(n\right)}\right) \tag{35}$$

Where M and N are number of rows and columns of both the images.

Entropy: The quantity of information that the image comprises is known as. It can be used for calculating the accuracy of the image fused from the output. The entropy will be established if the pixel-level likelihood density (p) is established. If the entropy is greater, then fusion is effective (Bhateja et al., 2015).

$$Entropy=-\sum_{i=0}^{K-1}p\left(mi\right)\log p\left(mi\right) \tag{36}$$

Edge based similarity measure ($Q^{AB/F}$): It can be used to calculate the dimensions of the edges of a fused photograph. Q's value for a good quality fused image is equivalent to 1. A variety of methods are added to get the image's edge knowledge such as basic algorithm for edge detection, local gradients, and much more [34]. It is determined with equation below.

	FSIM	ENTROPY	PSNR	SSIM	STD	$Q^{AB/F}$	MI	CC
PSO	0.991425	22.640391	34.39331	0.94834	0.137244	0.594891	3.30639	0.59489
QPSO	0.960303	22.679535	34.58154	0.949456	0.152098	0.604217	3.34325	0.60422
HBMO	0.942479	22.689466	34.58518	0.953553	0.183669	0.683029	3.34592	0.68303
Proposed	0.944423	22.881475	34.71021	0.976054	0.165419	0.699309	3.34999	0.69854

$$Q^{AB/F} = \frac{\sum_{i=1}^{x}\sum_{j=1}^{y} Qa\left(i,j\right)Wa\left(i,j\right) + Q\left(i,j\right)Wb\left(i,j\right)}{\sum_{i=1}^{x}\sum_{j=1}^{y} Wa\left(i,j\right) + Wb\left(i,j\right)} \tag{37}$$

Where $Qa(i,j)=Qa_g(x,y)Qa_\alpha(x,y)$, $Qb(i,j)=Qb(x,y)Qb_\alpha(x,y)$ (38)

Correlation coefficient (CC): Using this function, the closeness between the reference image and the fused image is determined. If the reference image and the fused image are similar then the coefficient of similarity is almost equal to 1 [34]. If there is an actual discrepancy between the fused image and the reference image, then the correlation coefficient value would be less than 1.

$$C = \frac{\sum_{i=1}^{j}\left(m_i - M\right)}{\sqrt{\sum_{i=1}^{j}\left(m_i - M\right)^2 \sum_{i=1}^{j}\left(n_i - N\right)^2}} \tag{39}$$

Where M and N are mean values of corresponding images.

DISCUSSIONS

In this section experiments on CT/MRI Image Fusion is explained with different diseases.

Neoplastic disease: Neoplastic diseases are conditions which trigger growth of the tumors. It is the type of tumor that is triggered by excessive cell growth in the brain. They may be benevolent and malicious. Non-cancerous benign tumors develop gradually and disperse fewer to other tissues. Malignant tumors are cancerous and can spread to other organs or tissues. If not identified early, this may be life-threatening. The early detection of such development cannot contribute to cancer. If this development is malignant, it can expand at an accelerated pace to the other areas of the brain, contributing to cancer. From figure 6, the proposed algorithm recognizes certain tumor growth better than others, and table 1 indicates the efficiency of the proposed algorithm in FSIM, SSIM, Entropy, PSNR, $Q^{AB/F}$ and MI.

Cerebrovascular disease: Cerebrovascular disorder applies to diseases that may induce stroke and disrupt blood supply across the brain. The most important risk factor for stroke and cerebrovascular disorder is hypertension (high blood pressure). This illness, induced fatally or briefly by any of the factors such as ischemia, brain field, excessive loss and presence of more than two blood vessels in pathological processes. This involves aneurysms, vertebral stenosis, carotid stenosis and stroke, intracranial stenosis and vascular malformations. Many diseases may be avoided by improvements in medicine and lifestyle. Blood thinners and other modalities are used for treating strokes, including surgery. Figure 7 indicates the success of the proposed algorithm in the visual output and Table 2 indicates is stronger in all proposed calculated parameters.

Figure 6. a) input images b) Segmented images: Fused images c) with PSO d) with QPSO e) with HBMO f) with hGAPSO-SOS

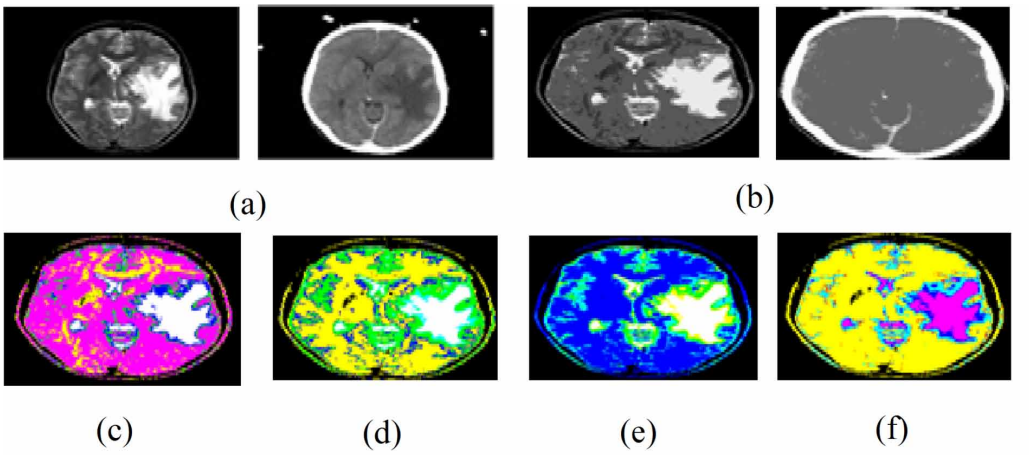

Figure 7. a) input images b) Segmented images: Fused images c) with PSO d) with QPSO e) with HBMO f) with hGAPSO-SOS

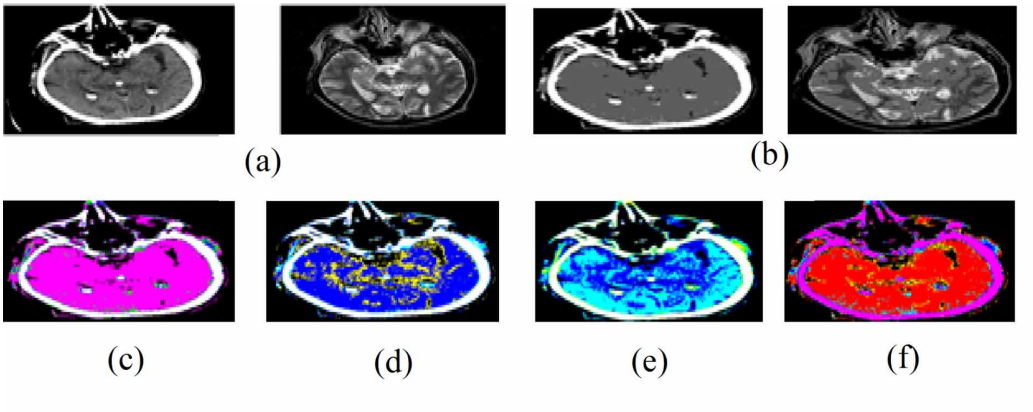

Alzheimer disease: Alzheimer's disease is an irreversible progressive brain disorder which gradually destroys memory and thinking abilities, the ability to perform even simple tasks. Typically first appears in the mid-60s. There is no cure for this condition, but medication can help delay disease progression and improve quality of life. In general, this disease is diagnosed by manually or eye tracing or MRI scan or CT scan checking of the metal stability. A slight structural variation in the brain contributes to disease, and it is a major challenge for researchers to recognize such a small difference. In this article, MRI and CT scan images are fused for better identification of small brain differences that leads to early diagnosis of Alzheimer's. T1-Weighted MR image of 70-year-old man and 73-year-old T2-Weighted MR images are considered for performance testing of proposed method. Figure 8 well describes the qualitative outcome of the proposed algorithm. From the figure, as compared with other algorithms, the visual output of Alzheimer's disease is better with proposed. The proposed quantitative findings are as shown in table 3. It shows dominance in every aspect.

Table 3: Set –C: Alzheimer disease

	FSIM	ENTROPY	PSNR	SSIM	STD	$Q^{AB/F}$	MI	CC
PSO	0.336717	21.390594	32.82359	0.911531	0.777079	0.719411	3.1012	0.71941
QPSO	0.444859	21.405167	32.83409	0.937020	0.444859	0.720572	3.1255	0.72057
HBMO	0.660098	21.485016	32.85253	0.951837	0.660980	0.725686	3.1454	0.72569
Proposed	0.784578	21.499874	32.88978	0.961254	0.454554	0.758797	3.1965	0.75687

Fatal disease: There is no treatment for a fatal illness that eventually ends in the patient's death. Death can occur within a few hours to several years, depending on the disease in question. Some fatal illnesses include cancer, serious heart disease, AIDS, dementia, etc. As there is no cure, only supportive and palliative care can be offered to the patients. Pick's illness is regarded as a fatal disease in this article. Pick's disease is a genetic disorder that leads to memory loss, decreased rates of thought, reminiscent of human language and odd behavior. The explanation for that is some mild brain tissue trauma. By fusing CT and MRI images, this can be established and was successfully achieved with the proposed method and compared the findings with other soft computing techniques. The proposed method effectiveness in fusing the images is observed in the form table 4 and in figure 9.

Table 4: Set –D: Fatal disease

	FSIM	ENTROPY	PSNR	SSIM	STD	$Q^{AB/F}$	MI	CC
PSO	0.307900	22.177216	32.56973	0.897339	0.437479	0.742869	3.54065	0.74287
QPSO	0.437479	22.254970	32.63030	0.920576	0.833801	0.756198	3.54868	0.75620
HBMO	0.693950	22.278068	32.78759	0.924099	0.307951	0.768028	3.59584	0.76803
Proposed	0.896587	22.457811	32.96587	0.945784	0.854754	0.789745	3.63698	0.79874

Sarcoma disease: Sarcoma is a malignant tumor and is a rare form of cancer. Sarcomas develop in cells of the connective tissue such as skin, blood vessels, nerves, bones, muscles and cartilage. They are surgically treated to remove the tumor and chemotherapy and radiotherapy. Sarcomas appear to be incurable and can be fatal. The visual fused image quality obtained with hGAPSO-SOS from figure 10 is much greater than the fused images obtained with PSO, QPSO and HBMO. The green color regions in Figure 10(f) indicate the regions affected by the tumor that are highlighted with the hGAPSO-SOS proposed. The method proposed is stronger not only in terms of visual efficiency but also in other measuring parameters of fusion, as shown in table 5.

It is found from the above discussions, findings and experiments that the proposed hGAPSO-SOS provides advanced quantities of mutual knowledge (MI) through image thresholding and Scale-Invariant Function Transform. The experimental results indicate that there is substantial quantitative progress in the proposed fusion technique than that of the current fusion techniques. This fusion algorithm is tested for applications in medical imaging, and is also well suited for other applications such as remote sensing and area growth. The proposed technique can be used in applications for satellite imaging, such as weather forecasting, forest destruction, and application for object tracking. The proposed technique can be used in applications for satellite imaging, such as weather forecasting,

Table 5: Set –E: Sarcoma disease

	FSIM	ENTROPY	PSNR	SSIM	STD	$Q^{AB/F}$	MI	CC
PSO	0.21906	21.23275	33.691	0.89593	0.24321	0.649	2.8722	0.6490
QPSO	0.24321	21.25676	33.708	0.90873	0.32883	0.6583	2.8922	0.6583
HBMO	0.32883	21.39504	33.767	0.92194	0.21906	0.6615	2.8956	0.6615
Proposed	0.401254	21.69874	33.865	0.93258	0.36984	0.68745	2.9999	0.6895

Figure 8. a) input images b) Segmented images: Fused images c) with PSO d) with QPSO e) with HBMO f) with hGAPSO-SOS

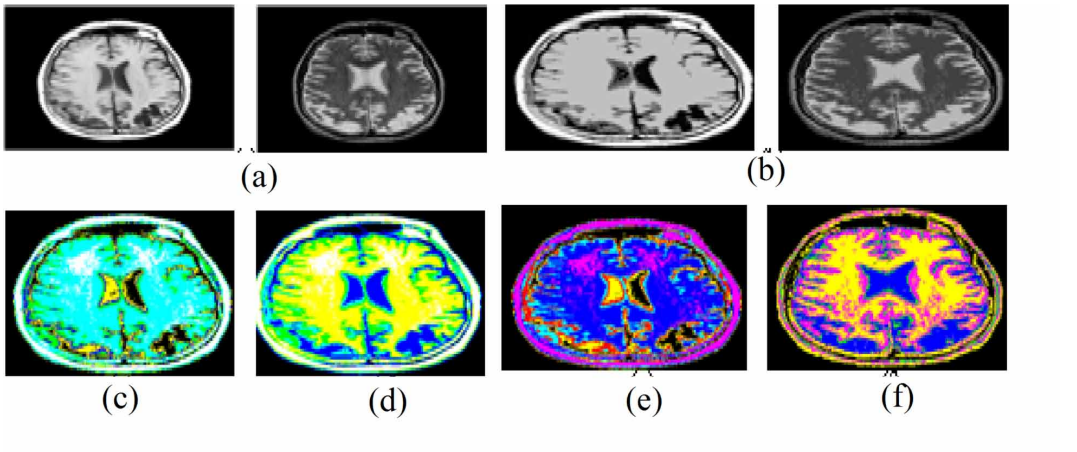

Figure 9. a) input images b) Segmented images: Fused images c) with PSO d) with QPSO e) with HBMO f) with hGAPSO-SOS

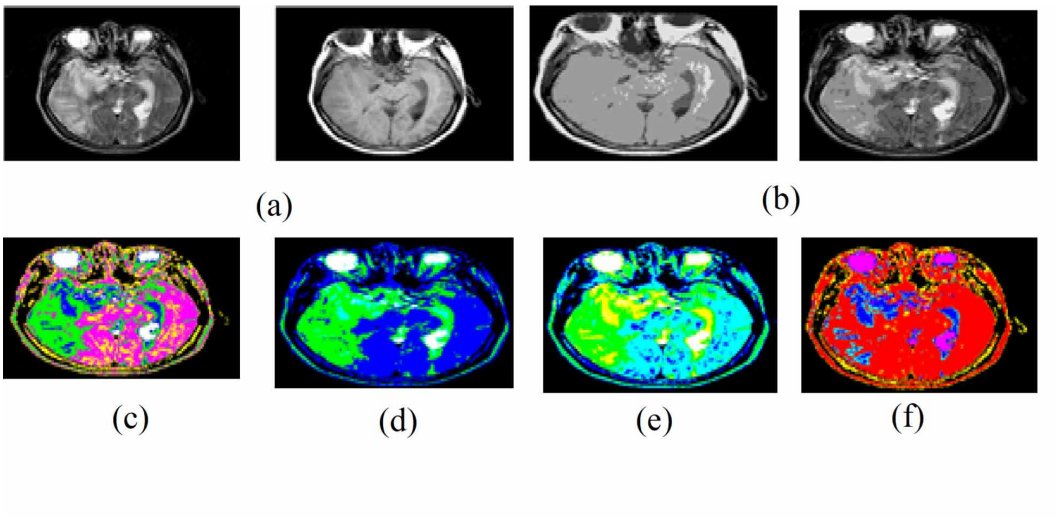

Figure 10. a) input images b) Segmented images: Fused images c) with PSO d) with QPSO e) with HBMO f) with hGAPSO-SOS

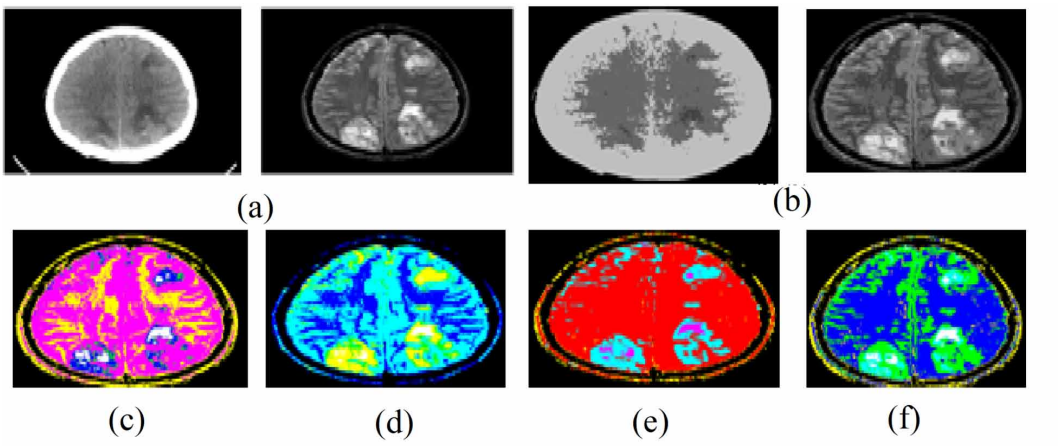

forest destruction, and application for object tracking. The proposed algorithm overcomes PSO, QPSO and HBMO constraints.

CONCLUSIONS

Two MRI images are merged in this paper to help identify diseases such as neoplastic disease, cerebrovascular disease, Alzheimer's disease, fatal disease, sarcoma disease. The two images are segmented by assuming Renyi entropy as an objective function on the basis of 2-D histogram with hGAPSO-SOS. It is used to get optimum thresholds for better segmentation. The segmented regions of both images are extracted using the Scale Invariant Feature Transform (SIFT), and both images are fused based on Fuzzy set fusion laws of type-2 interval. From the experiments, the proposed algorithm is better than other algorithms in terms of visual quality for diagnosing diseases and better in terms of mutual knowledge, Edge-based similarity measurement and correlation coefficient. The proposed methods further improved with the recent deep learning algorithms.

CONFLICTS OF INTEREST

None

REFERENCES

Al-Tayyan, A., Assaleh, K., & Shanableh, T. (2017). Decision-level fusion for single-view gait recognition with various carrying and clothing conditions. *Image and Vision Computing*, *61*, 54–69. doi:10.1016/j.imavis.2017.02.004

Bhateja, V., Patel, H., Krishn, A., Sahu, A., & Lay-Ekuakille, A. (2015). Multimodal medical image sensor fusion framework using cascade of wavelet and contourlet transform domains. *IEEE Sensors Journal*, *15*(12), 6783–6790. doi:10.1109/JSEN.2015.2465935

Cheng, M. Y., & Prayogo, D. (2014). Symbiotic organisms search: A new metaheuristic optimization algorithm. *Computers & Structures*, *139*, 98–112. doi:10.1016/j.compstruc.2014.03.007

Chiranjeevi, K., & Jena, U. (2017). Hybrid gravitational search and pattern search–based image thresholding by optimising Shannon and fuzzy entropy for image compression. *International Journal of Image and Data Fusion*, *8*(3), 236–269. doi:10.1080/19479832.2017.1338760

Chiranjeevi, K., & Jena, U. (2018). SAR image compression using adaptive differential evolution and pattern search based K-means vector quantization. *Image Analysis & Stereology*, *37*(1), 35–54. doi:10.5566/ias.1611

Chiranjeevi, K., Jena, U., & Prasad, P. M. K. (2017). Hybrid cuckoo search based evolutionary vector quantization for image compression. In *Artificial Intelligence and Computer Vision* (pp. 89–114). Springer. doi:10.1007/978-3-319-46245-5_7

Choi, M., Kim, R. Y., Nam, M. R., & Kim, H. O. (2005). Fusion of multispectral and panchromatic satellite images using the curvelet transform. *IEEE Geoscience and Remote Sensing Letters*, *2*(2), 136–140. doi:10.1109/LGRS.2005.845313

Dutta, P. (2017). Decision making in medical diagnosis via distance measures on interval valued fuzzy sets. *International Journal of System Dynamics Applications*, *6*(4), 63–83. doi:10.4018/IJSDA.2017100104

El-Hoseny, H. M., Abd El-Rahman, W., El-Rabaie, E. S. M., Abd El-Samie, F. E., & Faragallah, O. S. (2018). An efficient DT-CWT medical image fusion system based on modified central force optimization and histogram matching. *Infrared Physics & Technology*, *94*, 223–231. doi:10.1016/j.infrared.2018.09.003

Galli, B. J. (2018). Application of system engineering to project management: How to view their relationship. *International Journal of System Dynamics Applications*, *7*(4), 76–97. doi:10.4018/IJSDA.2018100105

Ghassemian, H. (2016). A review of remote sensing image fusion methods. *Information Fusion*, *32*, 75–89. doi:10.1016/j.inffus.2016.03.003

Grosan, C., & Abraham, A. (2011). *Intelligent systems*. Springer. doi:10.1007/978-3-642-21004-4

Haddadpour, M., Daneshvar, S., & Seyedarabi, H. (2017). PET and MRI image fusion based on combination of 2-D Hilbert transform and IHS method. *Biomedical Journal*, *40*(4), 219–225. doi:10.1016/j.bj.2017.05.002 PMID:28918910

Harris, C. G., & Stephens, M. (1988, August). A combined corner and edge detector. In Alvey vision conference (Vol. 15, No. 50, pp. 10-5244). doi:10.5244/C.2.23

He, Y., Deng, G., Wang, Y., Wei, L., Yang, J., Li, X., & Zhang, Y. (2018). Optimization of SIFT algorithm for fast-image feature extraction in line-scanning ophthalmoscope. *Optik (Stuttgart)*, *152*, 21–28. doi:10.1016/j.ijleo.2017.09.075

Jin, X., Jiang, Q., Yao, S., Zhou, D., Nie, R., Hai, J., & He, K. (2017). A survey of infrared and visual image fusion methods. *Infrared Physics & Technology*, *85*, 478–501. doi:10.1016/j.infrared.2017.07.010

Karri, C., & Jena, U. (2016). Fast vector quantization using a Bat algorithm for image compression. *Engineering Science and Technology, an International Journal, 19*(2), 769-781.

Lang, J., & Hao, Z. (2014). Novel image fusion method based on adaptive pulse coupled neural network and discrete multi-parameter fractional random transform. *Optics and Lasers in Engineering*, *52*, 91–98. doi:10.1016/j.optlaseng.2013.07.005

Li, L., & Li, D. (2008). Fuzzy entropy image segmentation based on particle swarm optimization. *Progress in Natural Science*, *18*(9), 1167–1171. doi:10.1016/j.pnsc.2008.03.020

Lowe, D. G. (1999, September). Object recognition from local scale-invariant features. In *Proceedings of the seventh IEEE international conference on computer vision* (Vol. 2, pp. 1150-1157). IEEE. doi:10.1109/ICCV.1999.790410

Majhi, S. K. (2018). An efficient feed foreword network model with sine cosine algorithm for breast cancer classification. *International Journal of System Dynamics Applications*, *7*(2), 1–14. doi:10.4018/IJSDA.2018040101

Mendel, J. M., & John, R. B. (2002). Type-2 fuzzy sets made simple. *IEEE Transactions on Fuzzy Systems*, *10*(2), 117–127. doi:10.1109/91.995115

Mousa, M. E., Ebrahim, M. A., & Hassan, M. M. (2015). Stabilizing and swinging-up the inverted pendulum using PI and PID controllers based on reduced linear quadratic regulator tuned by PSO. *International Journal of System Dynamics Applications*, *4*(4), 52–69. doi:10.4018/IJSDA.2015100104

Naidu, V. P. S., & Raol, J. (2008). Pixel-level image fusion using wavelets and principal component analysis. *Defence Science Journal*, *58*(3), 338–352. doi:10.14429/dsj.58.1653

Naugle, A. B., Backus, G. A., Tidwell, V. C., Kistin-Keller, E., & Villa, D. L. (2019). A Regional Model of Climate Change and Human Migration. *International Journal of System Dynamics Applications*, *8*(1), 1–22. doi:10.4018/IJSDA.2019010101

Nirmala, D. E., & Vaidehi, V. (2015, March). Comparison of Pixel-level and feature level image fusion methods. In *2015 2nd international conference on computing for sustainable global development (INDIACom)* (pp. 743-748). IEEE.

Petrovic, V. S., & Xydeas, C. S. (2004). Gradient-based multiresolution image fusion. *IEEE Transactions on Image Processing*, *13*(2), 228–237. doi:10.1109/TIP.2004.823821 PMID:15376943

Rokbani, N., Kromer, P., Twir, I., & Alimi, A. M. (2020). A Hybrid Hierarchical Heuristic-ACO With Local Search Applied to Travelling Salesman Problem, AS-FA-Ls. *International Journal of System Dynamics Applications*, *9*(3), 58–73. doi:10.4018/IJSDA.2020070104

Saafan, M. M., Abdelsalam, M. M., Elksas, M. S., Saraya, S. F., & Areed, F. F. (2017). An adaptive neuro-fuzzy sliding mode controller for MIMO systems with disturbance. *Chinese Journal of Chemical Engineering*, *25*(4), 463–476. doi:10.1016/j.cjche.2016.07.021

Sarkar, S., & Das, S. (2013). Multilevel image thresholding based on 2D histogram and maximum Tsallis entropy—A differential evolution approach. *IEEE Transactions on Image Processing*, *22*(12), 4788–4797. doi:10.1109/TIP.2013.2277832 PMID:23955760

Wan, T., Zhu, C., & Qin, Z. (2013). Multifocus image fusion based on robust principal component analysis. *Pattern Recognition Letters*, *34*(9), 1001–1008. doi:10.1016/j.patrec.2013.03.003

Xu, Z. (2014). Medical image fusion using multi-level local extrema. *Information Fusion*, *19*, 38–48. doi:10.1016/j.inffus.2013.01.001

Yang, S., Wang, M., Lu, Y., Qi, W., & Jiao, L. (2009). Fusion of multiparametric SAR images based on SW-nonsubsampled contourlet and PCNN. *Signal Processing*, *89*(12), 2596–2608. doi:10.1016/j.sigpro.2009.04.027

Yang, Y., Que, Y., Huang, S., & Lin, P. (2016). Multimodal sensor medical image fusion based on type-2 fuzzy logic in NSCT domain. *IEEE Sensors Journal*, *16*(10), 3735–3745. doi:10.1109/JSEN.2016.2533864

Zadeh, L. A. (1965). Fuzzy sets. *Information and Control*, *8*(3), 338–353. doi:10.1016/S0019-9958(65)90241-X

Srikanth M. V. is a Ph.D student at Jawaharlal Nehru Technological University,Kakinada, INDIA, he has around 16 years of experience in teaching and his area of interest includes image fusion and computer vision.

V. V. K. D. V. Prasad is a Ph.D graduate from Jawaharlal Nehru Technological University, Kakinada, India; he has around 25 years of experience in teaching and his area of interest includes image fusion and computer vision.

K. Satya Prasad received a B Tech. degree in Electronics and Communication Engineering from JNTU college of Engineering, Anantapur, Andhra Pradesh, India in 1977 and an M.E. degree in Communication Systems from the Guindy College of Engineering, Madras University, Chennai, India in 1979 and a Ph.D from Indian Institute of Technology, Madras in 1989. He started his teaching carrier as Teaching Assistant at Regional Engineering College, Warangal in 1979.He joined JNT University, Hyderabad as Lecturer in 1980 and served in different constituent colleges viz., Kakinada, Hyderabad and Anantapur and at different capacities viz., Associate Professor, Professor, Head of the Department, Vice Principal and Principal. In JNTUK University he served as Director of Evaluation, Director IST and Rector. He has published more than 250 technical papers in various National & International Conferences and Journals and authored Four Text books. He has guided 33 PhD scholars and, at present, the 20 scholars who are working with him. His areas of Research include Communications, Signal Processing, Image Processing, Neural Networks & Ad-hoc wireless networks etc. Dr Prasad was a recipient of Andhra Pradesh State Teacher Award in 2009 and received different awards at the national level. Dr Prasad is a Fellow member of various professional bodies like IEEE, IETE, IE (I), and ISTE. After retiring from JNTUK service, Prasad worked as a Pro Vice Chancellor of KL University. At present he is working as Rector of Vignan's Foundation for Science, Technology and Research, Vadlamudi, Guntur, AP.